J|A|C|S
ARTICLES
Published on Web 07/24/2002

1,8-Naphthalimides in Phosphorescent Organic LEDs: The Interplay between Dopant, Exciplex, and Host Emission

Dmitry Kolosov,[†] Vadim Adamovich,[†] Peter Djurovich,[†] Mark E. Thompson,*[,†] and Chihaya Adachi[‡]

Contribution from the Department of Chemistry, University of Southern California, Los Angeles, California 90089, Department of Photonics Materials Science, Chitose Institute of Science and Technology, 758-65 Bibi, Chitose 066-8655, Japan

Received March 28, 2002

Abstract: Four different 1,8-naphthalimide derivatives were examined in phosphorescent organic light emitting diodes (OLEDs), i.e., 1,8-naphthalimide, *N*-phenyl-1,8-naphthalimide, *N*-2,6-dibromophenyl-1,8-naphthalimide (niBr), and bis-*N*,*N*-1,8-naphthalimide. Photoluminescence from all four naphthalimides have violet-blue fluorescence and phosphorescent bands between 550 and 650 nm (visible at 77 K). While all four compounds gave good glassy films when doped with a phosphorescent dopant, only the niBr films remained glassy for extended periods. OLED studies focused on niBr, with two different architectures. One OLED structure (type 1) had the niBr layer as a doped luminescent layer and an undoped niBr layer to act as a hole-blocking layer. The alternate structure (type 2) utilizes a doped CBP layer as the luminescent layer and the niBr layer is used as a hole-blocking layer only (CBP = 4,4′-*N*,*N*′-dicarbazolylbiphenyl). Type 1 and 2 OLEDs were prepared with green, yellow, and red emissive phosphorescent dopants (Irppy, btIr, and btpIr, respectively). The dopants were organometallic Ir complexes, previously shown to give highly efficient OLEDs. Of the three dopants, the btpIr-based OLEDs showed the best device performance in both structures (peak efficiencies for type 2: 3.2% and 2.3 lum/W at 6.3 V; type 1: 1.7% and 1.3 lm/W at 6.1 V). The green and yellow dopants gave very similar performance in both type 1 and 2 devices (peak efficiencies are 0.2−0.3%), which were significantly poorer than the btpIr-based OLEDs. The emission spectrum of the btIr- and btpIr-based devices (type 1 and 2) are the same as the solution photoluminescence spectrum of the dopant alone, while the Irppy device gives a broad red emission line (λ_{max} = 640 nm). The red Irppy·niBr emission line is assigned to an Irppy·niBr exciplex. The type 2 Irppy-based device gave a voltage-dependent spectrum, with the red emission observed at low bias (4−8 V), switching over to strong green emission as the bias was raised. All other devices showed bias-independent spectra. Estimates of HOMO, LUMO, and excited-state energies (dopant, niBr, and exciplex) were used to explain the observed spectral properties of these devices. btpIr-based devices emit efficiently from isolated dopant states (external efficiencies = 3.2 %, 2.3 lum/W). Irppy-based devices emit only from exciplex states, with low efficiency (external efficiency = 0.3%). btIr·niBr films have very similar energies for the dopant, exciplex, and niBr triplet states, such that relaxation can go through any of these states, leading to low device efficiency (external efficiency = 0.4%). High device efficiency is achieved only when dopant emission is the dominant pathway for relaxation, since exciplex and niBr triplet states give either weak or no electroluminescence.

Introduction

A great deal of experimental effort has focused on developing new materials for organic electronic and optoelectronic applications.[1] In many cases, breakthroughs in device performance have been tied directly to the use of new materials. A good example of this is seen in organic light-emitting diodes (OLEDs). Significantly improved device performance was realized for OLEDs when aluminum-tris(8-hydroxyquinolate), Alq_3, was introduced as an electron-transporting material.[2] Since the initial report of Alq_3-based OLEDs, it has been the most heavily studied electron transporter for OLEDs. To be useful as an electron transporter in an OLED, a given material must be chemically and thermally stable and have an electron-deficient π-system. In addition to Alq_3, metal complexes of metals other than Al have proven useful as well.[2,3] A number of different organic molecules have also been used as electron transporters, including oxadiazoles,[4] triazoles,[5] phenanthrolines,[6] and carbazole derivatives.[7−11] This paper explores the use of naphthalimides as electron transporters and luminescence host materials

* To whom correspondence should be addressed. E-mail: met@usc.edu.
[†] University of Southern California.
[‡] Chitose Institute of Science & Technology.

(1) Alivisatos, A. P.; Barbara, P. F.; Castleman, A. W.; Chang, J.; Dixon, D. A.; Klein, M. L.; McLendon, G. L.; Miller, J. S.; Ratner, M. A.; Rossky, P. J.; Stupp, S. I.; Thompson, M. E. *Adv. Mater.* **1998**, *10*, 1297.

(2) Tang, C. W.; VanSlyke, S. A. *Appl. Phys. Lett.* **1987**, *51*, 913. Tang, C. W.; VanSlyke, S. A. *J. Appl. Phys.* **1989**, *65*, 3610. Tang, C. W. *1996 SID Int. Symp., Digest of Technical Papers*; SID, San Diego, 1996; p 181; *Information Display* **1996**, *10*, 16. Burrows, P. E.; Shen, Z.; Bulovic, V.; McCarty, D. M.; Forrest, S. R.; Cronin, J.; Thompson, M. E. *J. Appl. Phys.* **1996**, *79*, 7991.

for organic light-emitting diodes. The goal is both to evaluate these materials in high-efficiency device structures and to explore the relationship between the electronic properties of each host/dopant system and the device properties, such as OLED efficiency and the origin of the emitting state (i.e., host, dopant, or exciplex).

1,8-Naphthalimide compounds are an attractive class of electron-deficient organic materials for OLEDs. They have high electron affinities,[12] and related naphthalenetetracarboxylic diimide compounds have electron mobilities as high as 0.16 $cm^2/(V\ s)$.[13] 1,8-Naphthalimides can have wide energy gaps[14−18] and low reduction potentials,[19] making them good candidates for use as n-type materials in OLEDs. While many 1,8-naphthalimide derivatives have low luminescent efficiencies at room temperature, due to strong intersystem crossing to their triplet states,[16,17] 1,8-naphthalimides substituted at the 4 position with electron-donating groups can have high fluorescent quantum yields.[14,18]

Naphthalimides have been utilized in both small molecule[20−24] and polymer-based[12,25−28] OLEDs. The small molecule based devices, utilizing 4-amino-1,8-naphthalimides as light-emitting material, showed performance inferior to that of Alq_3-based OLEDs. Emission from intramolecular charge-transfer states contribute greatly to electroluminescence of these devices.[22−24] Doping an orange/red fluorescent dye (DCM) into a 4-amino-1,8-naphthalimide matrix shifted the electroluminescence (EL) spectra to correspond exactly to photoluminescence (PL) spectrum of DCM, but did not noticeably improve performance of the devices.[20] The authors concluded that there was no energy transfer from the naphthalimide matrix to DCM, but the dye molecules could efficiently trap charge carriers in the devices, leading to electron−hole recombination at the DCM dopants followed by DCM emission. OLEDs utilizing side-chain naphthalimide polymers showed that these materials affect the device charge transport properties significantly and, in particular, reduce the bias necessary for electroluminescence.[12,28]

Cleave et al. recently reported the doping of a phosphorescent dopant (i.e., platinum octaethyl porphyrin, PtOEP) into a naphthalimide side-chain polymer.[29] Efficient energy transfer from the polymer to PtOEP was observed. While the efficiencies of these devices were not high, the use of phosphorescent dopants has the potential of giving very high efficiency devices in both small molecule[30] and polymer-based[31] OLEDs.

The high electron affinities and ionization potentials of 1,8-naphthalimides suggest that they may be useful electron transport or hole-blocking materials in electrophosphorescent OLEDs. Although it appears that the triplet energy level of 1,8-naphthalimides (phosphorescence maxima near 540 nm)[16−18] may limit application of these materials as a host to orange and red dopants only, the recent successful demonstration of efficient electrophosphorescence from a device in which the host has lower triplet energy than the dopant[11] suggests the possibility of utilizing these materials for green or blue devices as well.

To investigate the potential of 1,8-naphthalimides in electrophosphorescent OLEDs, we have focused on the characterization of 1,8-naphthalimide-based OLEDs doped with highly emissive Ir-based complexes, i.e., bis(2-(2′-benzo[4,5-*a*]thienyl)-pyridinato-N,C3′) iridium (acetyl-acetonate) (btpIr),[10,33] bis(2-phenylbenzothiozolato-N,$C^{2'}$) iridium (acetyl-acetonate) (btIr),[32,33] and *fac*-tris(2-phenylpyridine) iridium (Irppy).[9] The molecular structures of the Ir phosphors and 1,8-naphthalimides investigated in this study are given in Figure 1. The emission maxima of these Ir phosphorescent complexes in dilute solutions are 612,[32] 557,[32] and 510 nm,[34] respectively, placing the dopant emissive states below, close to, and above the triplet energies of 1,8-naphthalimides. This choice of phosphorescent emitters

(3) Sapochak, L. S.; Burrows, P. E.; Thompson, M. E.; Forrest, S. R. *J. Phys. Chem.* **1996**, *100*, 17766. Shoustikov, A. A.; You, Y.; Thompson, M. E. *IEEE J. Sel. Top. Quantum Electron.* **1998**, *4* (1), 3. Burrows, P. E.; Forrest, S. R.; Thompson, M. E. *Curr. Opin. Solid State Mater. Sci.* **1997**, *2*, 236. Hamada, Y. *IEEE Trans. Electron Devices* **1997**, *44*, 1208. Li, Y.; Liu, Y.; Bu, W.; Lu, D.; Wu, Y.; Wang, Y. *Chem. Mater.* **2000**, *12*, 2672. Rothberg, L. J.; Lovinger, A. J. *J. Mater. Res.* **1996**, *11*, 3174.

(4) (a) Adachi, C.; Tokito, S.; Tsutsui, T.; Saito, S. *Jpn. J. Appl. Phys., Part 1*, **1988**, *27*, 713. (b) Brown, A. R.; Burroughes, J. H.; Greenham, N. C.; Friend, R. H.; Bradley, D. C.; Burn, P. L.; Kraft, A.; Holmes, A. B. *Appl. Phys. Lett.* **1992**, *61*, 2793.

(5) (a) Adachi, C.; Baldo, M.; Forrest, S. R.; Thompson, M. E. *Appl. Phys. Lett.* **2000**, *77* (6), 904. (b) Kido, J.; Hongawa, K.; Okuyama, K.; Nagai, K. *Jpn. J. Appl. Phys., Part 2* **1993**, *32*, L917.

(6) Nakada, H.; Kawami, S.; Nagayama, K.; Yonemoto, Y.; Murayama, R.; Funaki, J.; Wakimoto, T.; Imai, K. *Polym. Prepr. Jpn.* **1994**, *35*, 2450.

(7) Kozlov, V. G.; Parthasarathy, G.; Burrows, P. E.; Forrest, S. R.; You, Y.; Thompson, M. E. *Appl. Phys. Lett.* **1998**, *72* (2), 144.

(8) O'Brien, D. F.; Baldo, M. A.; Thompson, M. E.; Forrest, S. R. *Appl. Phys. Lett.* **1999**, *74* (3), 442.

(9) Baldo, M. A.; Lamansky, S.; Burrows, P. E.; Thompson, M. E.; Forrest, S. R. *Appl. Phys. Lett.* **1999**, *75* (1), 4.

(10) Adachi, C.; Baldo, M. A.; Forrest, S. R.; Lamansky, S.; Thompson, M. E.; Kwong, R. C. *Appl. Phys. Lett.* **2001**, *78* (11), 1622.

(11) Adachi, C.; Kwong, R. C.; Djurovich, P.; Adamovich, V.; Baldo, M. A.; Thompson, M. E.; Forrest, S. R. *Appl. Phys. Lett.* **2001**, *79*, 2082.

(12) Cacialli, F.; Friend, R. H.; Bouche, C. M.; Le Barny, P.; Facoetti, H.; Soyer, F.; Robin, P. *J. Appl. Phys.* **1998**, *83* (4), 2343.

(13) Katz, H. E.; Lovinger, A. J.; Johnson, J.; Kloc, C.; Siegrist, T.; Li, W.; Lin, Y.; Dodabalapur, A. *Nature* **2000**, *404*, 478.

(14) Alexiou, M. S.; Tychopoulos, V.; Ghorbanian, S.; Tyman, J. H.; Brown, R.; Brittain, P. *J. Chem. Soc., Perkin Trans. 2* **1990**, 837.

(15) Demeter, A.; Biczok, L.; Berces, T.; Wintgens, V.; Valat, P.; Kossanyi, J. *J. Phys. Chem.* **1993**, *97*, 3217.

(16) Wintges, V.; Valat, P.; Kossanyi, J.; Biczok, L.; Demeter, A.; Berces, T. *J. Chem. Soc., Faraday Trans.* **1994**, *90* (3), 411.

(17) Demeter, A.; Berces, T.; Bicsok, L.; Wintges, V.; Valat, P.; Kossanyi, J. *J. Phys. Chem.* **1996**, *100*, 2001.

(18) Wintges, V.; Valat, P.; Kossanyi, J.; Demeter, A.; Biczok, L.; Berces, T. *New J. Chem.* **1996**, *20*, 1149.

(19) Martin, E.; Weigand, R. *Chem. Phys. Lett.* **1998**, *288*, 52.

(20) Utsugi, K.; Takano, S. *J. Electrochem. Soc.* **1992**, *139* (12), 3610.

(21) Yin, S.; Liu, X.; Huang, W.; Li, W.; He, B. *Thin Solid Films* **1998**, *325*, 268.

(22) Su, J.; Xu, T.; Chen, K.; Tian, H. *Synth. Met.* **1997**, *91*, 249.

(23) Ni, W.; Su, J.; Chen, K.; Tian, H. *Chem. Lett.* **1997**, 101.

(24) Tian, H.; Su, J.; Chen, K.; Wong, T. C.; Gao, Z. Q.; Lee, C. S.; Lee, S. T. *Opt. Mater.* **2000**, *14*, 91.

(25) Hu, C.; Zhu, W.; Lin, W.; Tian, H. *Synth. Met.* **1999**, *102*, 1129.

(26) Bouche, C. M.; Le Barny, P.; Facoetti, H.; Soyer, F.; Robin, P. *J. Chim. Phys.* **1998**, *95*, 1351.

(27) Zhu, W.; Hu, C.; Chen, K.; Tian, H. *Synth. Met.* **1998**, *96*, 151.

(28) Yin, S.; Xu, Z.; Huang, W.; Zhang, F.; Hou, Y.; Wang, Y.; Xu, X. *Chin. J. Chem.* **1999**, *17* (5), 462.

(29) Cleave, V.; Tessler, N.; Yahioglu, G.; Le Barny, P.; Facoetti, H.; Boucton, N.; Friend, R. H. *Synth. Met.* **1999**, *102*, 939.

(30) (a) Baldo, M. A.; O'Brien, D. F.; You, Y.; Shoustikov, A.; Sibley, S.; Thompson, M. E.; Forrest, S. R. *Nature* **1998**, *395*, 151. (b) Baldo, M. A.; Lamansky, S.; Burrows, P. E.; Thompson, M. E.; Forrest, S. R. *Appl. Phys. Lett.* **1999**, *75*, 4. (c) Hong, Z.; Liang, C.; Li, R.; Li, W.; Zhao, D.; Fan, D.; Wang, D.; Chu, B.; Zang, F.; Hong, L.-S.; Lee, S.-T. *Adv. Mater.* **2001**, *13*, 1241. (d) Xie, H. Z.; Liu, M. W.; Wang, O. Y.; Zhang, X. H.; Lee, C. S.; Hung, L. S.; Lee, S.-T.; Teng, P. F.; Kwong, H. L.; Zheng, H.; Che, C.-M. *Adv. Mater.* **2001**, *13*, 1245.

(31) (a) Cleave, V.; Yahioglu, G.; Le Barny, P.; Friend, R. H.; Tessler, N. *Adv. Mater.* **1999**, *11*, 285. (b) McGehee, M. D.; Bergstedt, T.; Zhang, T.; Saab, A. P.; O'Regan, M. B.; Bazan, G. C.; Srdanov, V. I.; Heeger, A. J. *Adv. Mater.* **1999**, *11*, 1349. (c) Wu, A.; Yoo, D.; Lee, J. K.; Rubner, M. F. *J. Am. Chem. Soc.* **1999**, *121*, 4883. (d) Guo, T.-F.; Chang, S.-C.; Yang, Y.; Kwong, R. C.; Thompson, M. E. *Org. Electron.* **2000**, *1*, 15. (e) O'Brien, D. F.; Giebler, C.; Fletcher, R. B.; Cadby, A. J.; Palilis, L. C.; Lidzey, D. G.; Lane, P. A.; Bradley, D. D. C.; Blau, W. *Synth. Met.* **2001**, *116*, 379. (f) Lamansky, S.; Kwong, R. C.; Nugent, M.; Djurovich, P. I.; Thompson, M. E. *Org. Electron.* **2001**, *2*, 53. (g) Higgins, R. W. T.; Monkman, A. P.; Nothofer, H.-G.; Scherf, U. *J. Appl. Phys.* **2002**, *91*, 99.

(32) Lamansky, S.; Djurovich, P.; Murphy, D.; Abdel-Razzaq, F.; Lee, H.; Adachi, C.; Burrows, P. E.; Forrest, S. R.; Thompson, M. E. *J. Am. Chem. Soc.* **2001**, *123*, 4304

(33) Lamansky, S.; Djurovich, P.; Murphy, D.; Abdel-Razzaq, F.; Kwong, R.; Tsyba, I.; Bortz, M.; Mui, B.; Bau, R.; Thompson, M. E. *Inorg. Chem.* **2001**, *40*, 1704.

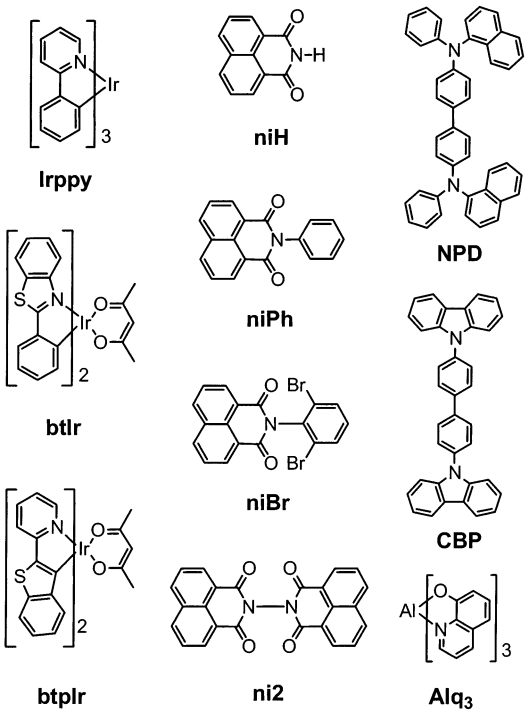

Figure 1. Molecular structures of phosphorescent dopant and 1,8-naphthylimide compounds investigated in this study.

allowed us to investigate how the differences in host−dopant triplet energies affect the color and efficiencies of the resulting electrophosphorescence devices. In this study we have seen both monomer and exciplex emission in the resulting devices. The highest device efficiencies were observed for OLEDs that emit from only dopant states (i.e., no exciplex or host emission is observed).

Experimental Section

Synthesis. The phosphorescent dopants used in this study (btpIr, btIr, and Irppy) were prepared by literature procedures.[32,33] Four different 1,8-naphthalimide derivatives were used in the study. 1,8-Naphthalimide (niH) was purchased from Sigma-Aldrich. *N*-Phenyl-1,8-naphthalimide (niPh) and *N*-2,6-dibromophenyl-1,8-naphthalimide (niBr) were prepared from 1,8-naphthalic anhydride and corresponding anilines according to a procedure by Rademacher et al.[35] Bis-*N*,*N*-1,8-naphthalimide (ni2) was prepared from 1,8-naphthalic anhydrate and hydrazine according to a procedure by Kuchkova et al.[36] All the reagents were purchased from Sigma-Aldrich and were used without further purification.

The four naphthalimides (niH, niPh, niBr, and ni2) were purified by thermal gradient sublimation in a vacuum (ca. 10^{-5} Torr). The characterization data for the three known compounds (niH, niPh, and ni2) matched the data given in the literature.[35−37] The characterization data for niBr are given below.

***N*-2,6-Dibromophenyl-1,8-naphthalimide.** Yield: 50%. ^{1}H NMR (acetone-d_6, 250 MHz), δ (ppm): 7.35−7.5 (t, 1H), 7.85−8.1 (m, 4H), 8.5−8.7 (m, 4H). MS, *m*/*z*: 352 (100), 214 (40), 126 (60). Anal. Calcd: C 50.04, H 1.98, N 3.23. Found: C 50.15, H 2.10, N 3.25.

Electrochemical Measurements. Cyclic voltametric measurements were recorded with an EG&G potentiostat/galvanostat model 28, at a scanning rate of 100 mV/s in deoxygenated *N*,*N*-dimethylformamide solutions containing 0.1 M tetrabutylammonium hexafluorophosphate. The potentials were recorded relative to a Ag/AgCl reference electrode with Pt wires used for both working and counterelectrodes. The data were recorded at room temperature.

Instrumental Measurements. Absorption spectra were recorded on an AVIV Model 14DS-UV-Vis-IR spectrophotometer (re-engineered Cary 14) and corrected for background due to solvent absorption. Emission spectra were recorded on a PTI QuantaMaster Model C-60SE spectrofluorometer with 928 PMT detector and corrected for detector sensitivity inhomogeneity. Triplet emission lifetimes were obtained at 77 K by exponential fit of emission decay[38] curves recorded on the PTI spectrofluorometer. The emission decay curves were recorded by fast (∼50 ms) closing of the excitation source shutters. The shutter closing was performed manually. The absorption spectra were taken in the dichloromethane solutions with optical densities of ∼0.1. The photoluminescence emission spectra were taken in dichloromethane and 2-methyltetrahydrofuran solutions.

The optical energy gaps for each of the materials were taken as the point of intersection of the normalized absorption and fluorescence spectra. All of the naphthalimide compounds examined here have small Stokes shifts between their absorption and fluorescence bands.

Thin films of naphthalimide compounds were examined with a Nikon Eclipse ME600 optical microscope equipped with a Pixera PVC 100C digital camera. Photoluminescence spectra of the films were taken with a PTI QuantaMaster Model C-60SE spectrofluorometer.

Ionization potentials were measured on neat thin films, using an AC-1 (Riken Keiki Co., Japan) UV photoelectron spectrometer.

OLED Fabrication and Testing. Organic layers were deposited onto precleaned transparent conductive indium−tin oxide glass substrates (ITO) by thermal evaporation method at 10^{-6} Torr vacuum. A hole-transport layer, a 350 Å thick layer of NPD (see Figure 1), was followed by a 250 Å thick emitting layer (an 1,8-naphthalimide derivative for type 1; 4,4′-*N*,*N*′-dicarbazolebiphenyl (CBP) for type 2) doped with 6−8% of a phosphorescent Ir complex. The emitting layer was followed by the hole-blocking (100 Å of the 1,8-naphthalimide derivative) and electron-injecting (200 Å of Alq_3) layers. A 1000 Å thick Mg:Ag cathode (10 mass % of Ag) was deposited on top of the organic films and capped with 500 Å of pure Ag. During device fabrication the vacuum was broken after deposition of the organic layers in order to install a cathode mask. All measurements on the devices were carried out in the air at room temperature.

Results and Discussion

Photophysical and Electrochemical Properties of Naphthalimides. A brief summary of photophysical data for 1,8-naphthalimide (niH), *N*-phenyl-1,8-naphthalimide (niPh), *N*-2,6-dibromophenyl-1,8-naphthalimide (niBr), and bis-*N*,*N*′-1,8-naphthalimide (ni2) is given in Table 1. Fluorescence from these complexes appears in the 340−460 nm range. The room-temperature emission spectra (predominantly fluorescence) are mirror images of the lowest energy absorption band; see Figure 2. These structured absorption and fluorescence bands indicate that a narrow distribution of vibrational states are involved in the electronic transition and that the geometry of the molecule in its relaxed Franck−Condon excited state is not very different from that of the ground-state molecule.[16] The spectroscopic properties of the singlet excited state of the *N*-alkyl-1,8-naphthalimides are controlled by the presence of a close-lying triplet excited state with n,π^* character, resulting in a high intersystem crossing efficiency (Φ_{isc} = 0.95 and 0.11 for niH and niPh, respectively).[16,18] The energy of the lowest triplet

(34) King, K. A.; Spellane, P. J.; Watts, R. J. *J. Am. Chem. Soc.* **1985**, *107*, 1432.
(35) Rademacher, A.; Markle, S.; Langhals, H. *Chem. Ber.* **1982**, *115*, 2927.
(36) Kuchkova, K. I.; Russo, A. G.; Selivanov, G. K.; Mshenskaya, T. A. *Izv. Akad. Nauk Moldavskoi SSR. Ser. Biol. Khim. Nauk* **1988**, *2*, 70.
(37) Day, J. C.; Govindaraj, N.; McBain, D. C.; Skell, P. S.; Tanko, J. M. *J. Org. Chem.* **1986**, *51*, 4959.
(38) Birks, J. B. *Photophysics of Aromatic Molecules*; Wiley-Interscience: London, 1970.

Table 1. Summary of Reported Photophysical Data for 1,8-Naphthalimide Compounds[a]

	$\lambda_{max\ f}$ (nm)	Φ_f	τ_f (nm)	$\lambda_{max\ ph}$ (nm)	τ_{ph} (s)	E°_{red} (V vs Ag/AgCl)	ref
niH	379	0.03	0.1	540−588−640	0.55	−1.25	16
niPh	386	0.0002	<0.05	542−588−640	0.55	−1.05	17,18
niBr	375	0.05	<1	536−584−636	0.54	−1.15	this work
ni2	380			540−584−636	0.84		this work

[a] $\lambda_{max\ f}$ = fluorescence emission maximum; Φ_f = fluorescence yield; τ_f = fluorescence lifetime; $\lambda_{max\ ph}$ = phosphorescence emission maximum; τ_{ph} = phosphorescence lifetime. All fluorescence data are given for solutions in acetonitrile at 300 K, phosphorescence data are given for 77 K in butyronitrile/butyl acetate glass (95:5, v:v). E°_{red} = the reduction potential, recorded cyclovoltametrically for DMF solutions.

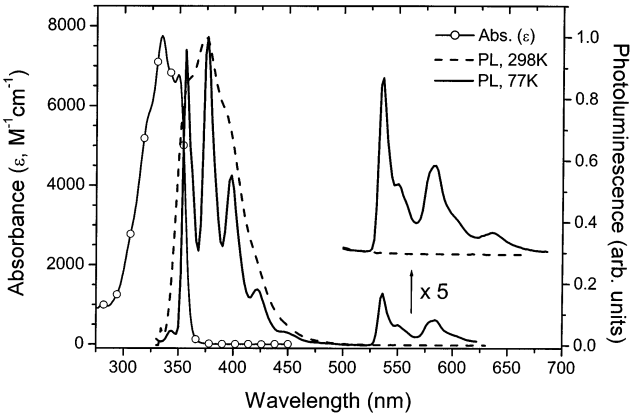

Figure 2. Absorption and emission spectra for niBr. Room-temperature spectra are for CH_2Cl_2 solution and the 77 K spectrum is a 2-MeTHF glass.

excited state is fairly independent of the substitution, whether on the dicarboximide nitrogen atom or on the naphthalene ring.[18]

Figure 2 shows the absorption and emission spectra at 300 K (dichloromethane solution) and photoluminescence at 77 K (2-methyltetrahydrofuran glass) for niBr. Photoluminescence spectra at 77 K in 2-methyltetrahydrofuran glasses are well structured, and emission from the triplet in the 550−650 nm region can be clearly seen. The measured lifetimes of these states are between 0.5 and 1 s, consistent with their assignment as organic triplet states. Dichloromethane solutions of any of the naphthalimides, cooled to 77 K, give broad structureless photoemission spectra, centered between 430 and 450 nm. The phosphorescent bands observed in THF glasses are not observed in these samples. The broad emission observed for frozen CH_2Cl_2 samples is most likely due to small molecular aggregates in the materials, formed by precipitation of the naphthalimide on cooling (see the following section).

1,8-Naphthalimides show fully reversible reduction waves in acetonitrile solutions. The reduction potentials for niH, niPh, and niBr are −1.25, −1.05, and −1.15 V (vs Ag/AgCl), respectively, consistent with the literature reports for niH[19] and niPh.[15] ni2 is too insoluble to obtain an accurate reduction potential. None of the naphthalimide compounds have a detectable oxidation wave in the solvents used here (acetonitrile and dichloromethane), putting it outside of the window available in these solvents (up to 2.0 V).

Both UV photoelectron spectroscopy (UPS) and electrochemical methods have been used to assess the HOMO energies (ionization potentials, IP) for molecular materials.[39] niBr has been examined by UPS and has a ionization potential that is outside the detectable energy limits of the UPS system used here, indicating that the IP is greater than 7 eV. While UPS is the preferred method for evaluating HOMO energies in OLED materials,[40−42] it was necessary to use electrochemical methods to estimate orbital energies of the naphthalimides. Since electrochemical oxidation was not observed for these materials, we have to rely on the reduction potentials to estimate the LUMO energies and use the LUMO to estimate the HOMO energies. In order for the electrochemical measurement to be used effectively, a reference compound must be used to convert the electrochemical reduction potential in solution to a LUMO energy, relative to vacuum. 4,4′-(*N*,*N*′-Dicarbazolyl)biphenyl (CBP) has been used extensively in OLEDs as a hole transporter and a host for phosphorescent dopants[7−11] and was used here as the reference for the naphthalimides. CBP shows a reversible reduction at −2.37 V (vs Ag/AgCl) and a LUMO energy of 2.7 eV. Using this potential, we place the LUMO levels of niH, niPh, and niBr at 3.8, 4.0, and 3.9 eV, respectively, relative to vacuum.

The HOMO energies for the naphthalimide compounds were calculated using the LUMO energy and optical energy gap for each of the naphthalimide compounds. The naphthalimdes give fluorescence spectra that are nearly mirror images of their long-wavelength absorption bands, indicating that the geometry of the molecule in its relaxed Franck−Condon excited state is not significantly different from that of the ground-state molecule. This makes it possible to use the optical energy gap (3.4 eV for niH, niPh, and niBr) as an estimate of the HOMO−LUMO gap for these naphthalimides.[41] Thus, the ionization energies of the naphthalimide HOMOs were calculated by adding the optical gaps for each of the naphthalimides to the corresponding LUMO energy. The HOMO energies estimated from the reduction potentials and optical gaps are 7.2, 7.4, and 7.3 eV, consistent with the lower limit set by our UPS measurements. It is important to note that the optical gap represents a lower limit of the carrier gap, since it is not corrected for the coulomb binding energy of the excited state. The error in this case gives the naphthalimide HOMO a lower ionization energy than its true HOMO energy. Since the estimated HOMO energies of the naphthalimides are well below any of the other materials considered here (vide infra), this error will not markedly change our picture.

The potential application of naphthalimides in OLEDs can be examined by comparing the naphthalimide HOMO and LUMO energies to the other OLED materials. We will discuss these states with reference to an energy level diagram of the isolated materials in their flatband conditions, as depicted in Figure 3. Although this is not intended to be a representation of the relevant energy levels under applied bias, it provides a suitable basis for the discussion of the relative energy levels. It is commonly accepted that the validity of usual band theory is limited for OLEDs, and charge conduction in the devices occurs through the hopping of charges between adjacent molecules with holes and electrons located at the molecular HOMOs and LUMOs, respectively. The ionization potential (IP) and electron

(39) Ishii, H.; Sugiyama, K.; Ito, E.; Seki, K. *Adv. Mater.* **1999**, *11*, 605.
(40) Richardson, D. E. *Inorg. Chem.* **1990**, *29*, 3213.
(41) The optical gap was defined at 0−0 transition, as the intersection of normalized absorption and emission spectra.
(42) Anderson, J. D.; McDonald, E. M.; Lee, P. A.; Anderson, M. L.; Ritchie, E. L.; Hall, H. K.; Hopkins, T.; Mash, E. A.; Wang, J.; Padias, A.; Thayumanav, S.; Barlow, S.; Marder, S. R.; Jabbour, G. E.; Shaheen, S.; Kippelen, B.; Peyghambarian, N.; Wightman, R. M.; Armstrong, N. R. *J. Am. Chem. Soc.* **1998**, *120*, 9646.

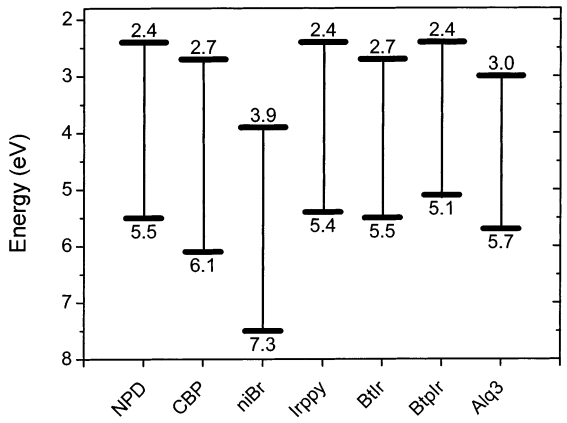

Figure 3. Positions of the HOMO and LUMO levels for the OLED materials. The energy for each orbital are listed below (HOMOs) or above (LUMOs) the appropriate bar. Energies were determined from UPS, optical, and electrochemical measurements, as described in the text.

Table 2. Oxidation and Reduction Potentials for Matrix and Dopant Materials in DMF[a]

compound	E°_{oxid} V vs Fc/Fc$^+$	E°_{red} V vs Fc/Fc$^+$	carrier gap (V)
CBP	0.50	−2.77	3.27
btpIr	0.36	−2.42	2.78
btIr	0.56	−2.15	2.71
Irppy	0.32	−2.69	3.01
niBr		−1.55	

[a] Fc = Fe(C_5H_5)$_2$. The potential for the Fc/Fc$^+$ couple falls at 0.40 V vs Ag/AgCl in DMF.

affinity (EA) of the material define positions of the HOMO and LUMO relative to the vacuum level. For NPD and Alq_3, the HOMO levels here were determined by UV photoemission spectroscopy (UPS), and the LUMOs estimated from IP values by subtracting the optical energy gap.[39,42]

For CBP, btpIr, btIr, and Irppy the HOMO energy was determined by UPS; however, the LUMO energy was estimated using the carrier gap, rather than the optical gap. The carrier gap for these compounds was measured electrochemically. All four of these compounds show fully reversible oxidation and reduction waves. The voltage difference between the waves gives a good estimate of the energy difference between the hole and electron states, i.e., the carrier gap. The redox potentials for these complexes are given in Table 2. This approach eliminates the inaccuracy associated with the use of the optical gap to approximate the carrier gap.

The HOMO levels for these naphthalimide compounds are very deep, suggesting that these materials may make good hole-blocking layers in OLEDs. The LUMO levels for the naphthalimides are also fairly deep, however, which may provide a barrier to electron injection into the luminescent zones of doped CBP-based devices. For this reason, two different types of OLEDs were examined, with naphthalimide- and CBP-doped emissive layers.

Thin Films of the 1,8-Naphthalimides. The first requirement a material must satisfy for it to be useful in OLEDs is that it must make high-quality thin films. Thin films of the naphthalimides were prepared by thermal evaporation. The qualities of the films were investigated by optical and atomic force microscopies. When niH, niPh, and ni2 were deposited directly onto quartz or onto a substrate precoated with an organic film (i.e., NPD), they did not give dense thin films. The surfaces of

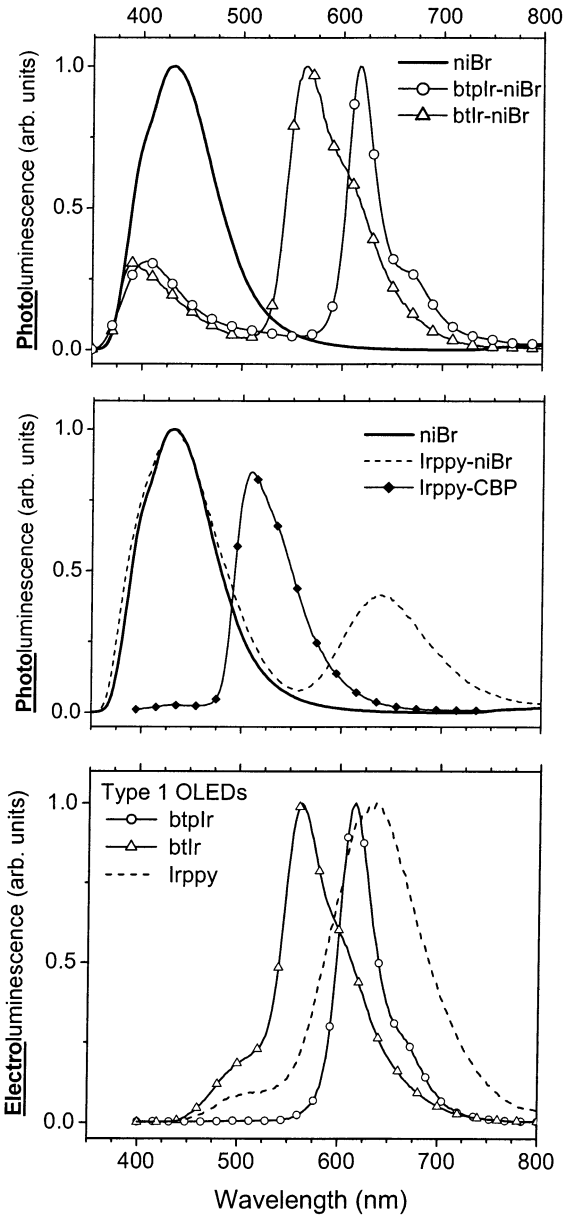

Figure 4. Photoluminescence (PL, top and middle) and electroluminescence (bottom) spectra of niBr and doped niBr films. The top plot shows the PL spectra for niBr, as well as the btpIr and btIr doped niBr films. The middle plot shows the PL spectra of niBr, Irppy doped niBr and the spectrum of Irppy doped into a matrix which does not interact significantly with the dopant (i.e., CBP, 1,4-*N*,*N*′-dicarbazolylbiphenyl). All PL spectra were obtained with an excitation wavelength of 325 nm. The bottom plot shows the electroluminescence spectra of type 1 devices, prepared with similarly doped niBr films.

the evaporated films appeared rough by optical microscopy, and the growth of crystals on a scale larger than 1 μm was observed. Co-deposition of niH, niPh, and ni2 with 6−8 mass % of any of the Ir dopants inhibited the crystallization processes in the films, such that freshly prepared samples appeared amorphous, but crystalline patterns developed in the films within hours. In contrast, niBr gave smooth, pinhole-free films, whether it was deposited pure or co-deposited with a phosphorescent dopant (i.e., btpIr, btIr, or Irppy).

Photoluminescence spectra of thin films of niBr, both doped and undoped, are shown in Figure 4. Emission from films of pure niBr is broad and featureless, with a λ_{max} of 436 nm. This

peak is red-shifted from the fluorescence observed for the THF solution by 60 nm. The thin film spectrum is very similar to that observed from dichloromethane solutions of niBr, cooled to 77 K. Wintges et al.[16] reported similar emission for *N*-methyl-1,8-naphthalimide and attributed it to delayed fluorescence from molecular aggregates, resulting from a triplet−triplet annihilation process. A similar process is most likely occurring in the neat niBr film as well.

When the niBr films are doped with 6−8 mass % of btpIr or btIr, energy transfer from the naphthalimide to the dopants is clearly evident. The photoluminescence spectra of these films feature emission bands with peaks at 566 and 620 nm for btIr- and btpIr-doped films, respectively, which are very similar to photoluminescence bands of these phosphors in dilute solution.[43] The excitation spectra for the doped films, taken at the maximum of the phosphor emission, have their maxima at the same wavelengths as the excitation spectrum for the undoped film. Both dopants have absorption energies low enough to quench the excited states of niBr. The ratios of the dopant/host peak emission intensities are similar for the btpIr- and btIr-doped films, suggesting similar energy-transfer rates for these two dopants.

When the niBr film is doped with 6−8 mass % of the green phosphor (Irppy), the film photoluminescence does not feature the monomer phosphor emission band, but shows a broad featureless band with a maximum at 640 nm in addition to the niBr band peaking at ∼430 nm (Figure 4). The excitation spectrum of the film, at the 640 nm emission line, is close to excitation spectra of niBr-doped films. The broad red emission is still present when the Irppy-doped film is excited at 400 nm (the ^{1}MLCT absorption band of the dopant), although the extinction coefficient for molecular niBr at this wavelength is negligibly small (Figure 4). The photoluminescence properties of pure and doped films described above are not specific to niBr; doped niH and niPh films showed similar behavior (i.e., a broad emission band at 640 nm for Irppy-doped films and dopant emission for btpIr- and btIr-doped films).

The lack of structure and low energy of the emission band for Irppy-doped niBr, niH, and niPh films, relative to their pure components (i.e., Irppy and the naphthalimide), suggest that the emitting state is an exciplex. An exciplex is an excited state whose wave function straddles two dissimilar molecules, one a net electron donor and the other an acceptor. Strong spin−orbit coupling of Ir presumably leads to the formation of a triplet exciplex. Emission from triplet exciplexes was first reported in the late 1960s[44] and has been reported for both organic and inorganic materials.[45−49] Zheng et al. proposed formation of an exciplex species, to explain emission of platinum(II) biphenyl dicarbonyl complex at low temperatures.[49] Mercer-Smith et al. demonstrated that palladium porphyrin triplet states form exciplexes with amines, which have a small degree of charge-transfer character and strongly resemble the uncomplexed porphyrin triplet in both lifetime and emission spectrum.[46] The exciplex state formed between Irppy and the naphthalimides shows a markedly different spectrum from either Irppy or the naphthalimide alone (see Figure 4), suggesting a high degree of charge transfer exists in the Irppy·naphthalimide exciplex.

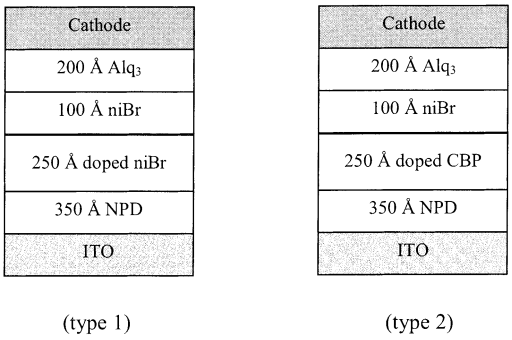

Figure 5. Type 1 and type 2 OLED architectures investigated here.

N-substituted 1,8-naphthalimides are known to be prone to exciplex formation due to the presence of a low-lying excited state of charge-transfer character.[18,19] Several authors, who investigated 4-amino-1,8-naphthalimides as light-emitting species in OLEDs, used exciplex formation to explain the observed EL spectra.[22−24] Hasharoni et al.[50] investigated intramolecular exciplexes in which 1,8-naphthalimide moieties behaved as the electron acceptors and concluded from EPR measurements that they have triplet character.

niBr-Based Phosphorescent OLEDs. Two different device architectures were used to evaluate the utility of the 1,8-naphthalimide complexes as electron-transporting and doped luminescent layers and as hole-blocking layers in electrophosphorescence OLEDs, as shown in Figure 5. In type 1 OLEDs, a 1,8-naphthalimide derivative was used to form both a 250 Å thick phosphor-doped emitting layer and a 100 Å thick hole-blocking layer. In type 2 devices, CBP was used as a host for the emitting layer and a 1,8-naphthalimide derivative was utilized as a 100 Å thick hole-blocking layer only. CBP has been used previously to make high-efficiency phosphorescent OLEDs.[8−11]

During initial studies, type 1 devices were fabricated for all four of the 1,8-naphthalimide derivatives investigated here (niH, ni2, niPh, niBr), doped with ca. 6 mass % btIr. All four naphthalimides gave working OLEDs with emission predominantly from the btIr dopant. However, niBr-based devices showed superior and more reliable performance, compared to niH-, niPh-, and ni2-based OLEDs, most likely due to better film-forming properties of niBr. For this reason, niBr was used for all further OLED studies.

Figure 4 shows electroluminescence spectra of type 1 niBr-based devices, doped with the three different phosphorescent Ir complexes. The OLED spectra are very similar to the PL spectra of the same doped films, except that the NiBr emission band of the PL spectra is absent in the EL spectra. Shoulders near 500 nm in the btIr- and Irppy-based devices are most likely

(43) Lamansky, S. Ph.D. Thesis, University of Southern California, 2001.
(44) Iwata, S.; Tanaka, J.; Nagakura, S. *J. Chem. Phys.* **1967**, *47* (7), 2203.
(45) Turro, N. J. *Modern Molecular Photochemistry*; University Science Books: Mill Valley, CA, 1991. Horvath, A.; Stevenson, K. L. *Coord. Chem. Rev.* **1996**, *153*, 57. Tears, D. K. C.; McMillin, D. R. B. *Coord. Chem. Rev.* **2001**, *211*, 195. Shizuka, H. *Pure Appl. Chem.* **1997**, *69*, 825. Lim, E. C. *Pure Appl. Chem.* **1993**, *65*, 1659. Sykora, A.; Sima, J. R. *Coord. Chem. Rev.* **1990** *107*, 1. Tero-Kubota, S.; Katsuki, A.; Kobori, Y. *J. Photochem. Photobiol. C: Photochem. Rev.* **2001**, *2*, 17. Shizuka, H.; Yamaji, M. *Bull. Chem. Soc. Jpn.* **2000**, *73*, 267.
(46) Mercer-Smith, J. A.; Sutcliffe, C. R.; Schmehl, R. H.; Whitten, D. G. *J. Am. Chem. Soc.* **1979**, *101*, 3995.
(47) Roundhill, D. M.; Gray, H. B. *Acc. Chem. Res.* **1989**, *22*, 55. Zipp, A. P.; *Coord. Chem. Rev.* **1988**, *84*, 47.
(48) Nagle, J. K.; Brennan, B. A. *J. Am. Chem. Soc.* **1988**, *110*, 5931. Herman, M. S.; Goldman, J. L. *J. Am. Chem. Soc.* **1989**, *111*, 9105.
(49) Zheng, G. Y.; Rillema, D. P. *Inorg. Chem.* **1998**, *37*, 1392.
(50) Hasharoni, K.; Levanon, H.; Greenfield, S. R.; Gosztola, D. J.; Scec, W. A.; Wasielewski, M. R *J. Am. Chem. Soc.* **1995**, *117*, 8055.

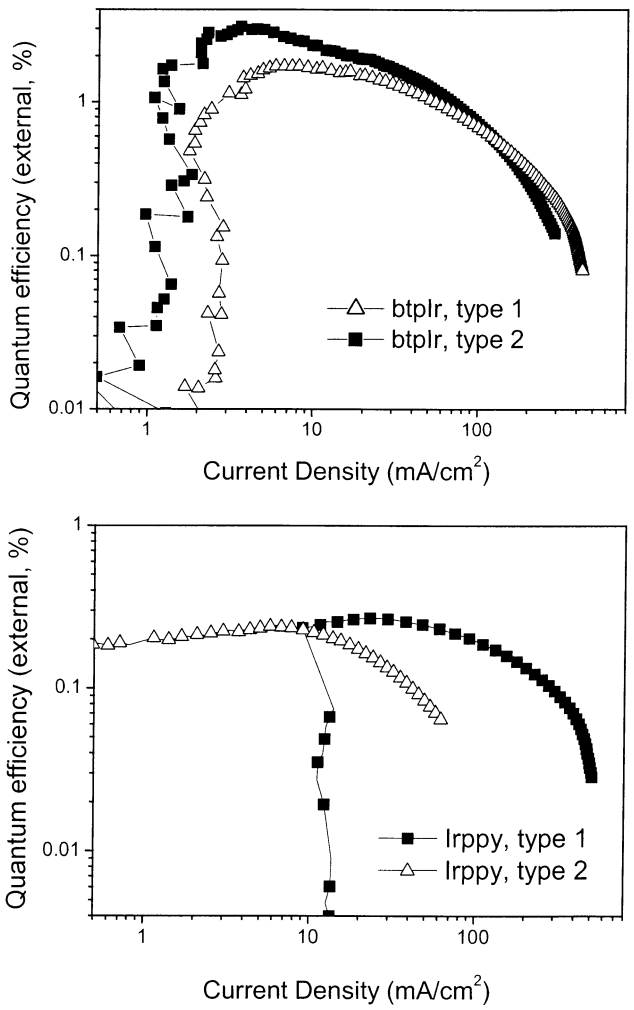

Figure 6. Quantum efficiency (photon per electron) vs current density for type 1 and 2 devices doped with btpIr (top) and Irppy-doped type 1 and type 2 devices (bottom).

due to imperfect hole blocking by the niBr layer, leading to weak Alq_3 emission.

The electroluminescence spectra of the btpIr-doped devices are identical to photoluminescence spectra of the phosphor in dilute solutions and in CBP-doped OLEDs[32] for both type 1 and 2 devices. The maximum quantum and luminescence efficiencies for the type 1 devices are 1.7% and 1.3 lm/W, which were achieved at 6.1 V (6.6 mA/cm^2, 400 Cd/m^2). The type 2 device performed significantly better, giving peak efficiencies of 3.2% and 2.3 lum/W at 6.3 V (4.5 mA/cm^2, 500 cd/m^2). Both type 1 and type 2 devices show the characteristic dropoff in QE vs current density (Figure 6). This is common and has been tied to triplet−triplet and polaron−exciton annihilation processes.[51−52] Maximum luminances of 3600 cd/m^2 (J = 190 mA/cm^2) and 3400 cd/m^2 (J = 105 mA/cm^2) were obtained for the type 1 and 2 devices, respectively.

The plots in Figure 7 give the optical power of the OLED in W/cm^2. It is customary to report OLED brightness in units that reflect the human eye response, i.e., cd/m^2. For btpIr emitting OLEDs a device power of 10^{-6} W/cm^2 corresponds to brightness of 2 cd/m^2. The turn-on voltages of the devices, defined as the

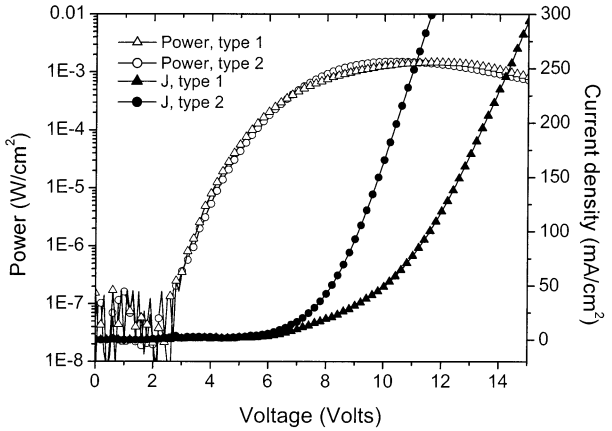

Figure 7. Luminance and current density vs voltage plots for type 1 and type 2 btpIr-doped OLEDs. 10^{-6} W/cm^2 ≈ 2 cd/m^2 for btpIr-based OLEDs.

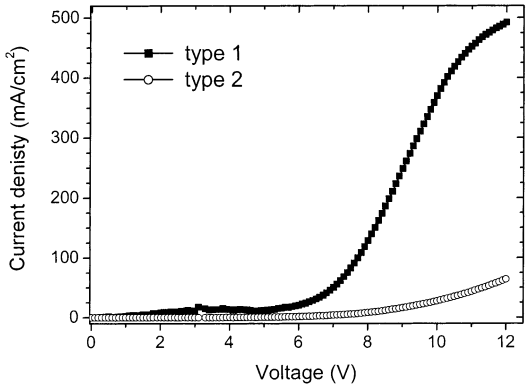

Figure 8. Current density vs voltage for Irppy-doped type 1 and 2 devices.

voltage at which the luminance is ∼10 times background noise level (ca. 2 cd/m^2), are 3 V in both cases. We were initially concerned about the deep LUMO level for niBr effectively trapping electrons, leading to poor electronic conduction across that layer. The low turn-on voltage and efficient charge conduction (i.e., high current at comparatively low voltage) demonstrate that this is not a problem for these devices, especially the type 2 devices.

A type 1 btIr-doped device gave quantum and luminance efficiencies of 0.4% and 0.6 lm/W (5.7 V, 34 mA/cm^2). The device had a maximum luminance of 6600 cd/m^2, at J = 430 mA/cm^2 and V = 10 V. The type 2 btIr-doped device gave very similar performance to that of the type 1 device. The peak quantum efficiency for this device was 0.3% (9 V). The turn-on voltages (3 V for type 1 and 4 V for type 2) and quantum efficiency versus current density characteristics for the btIr-based OLEDs are very similar to those of the corresponding btpIr-doped devices.

When the green emissive Irppy complex was used as a dopant in either type 1 or type 2 devices, the resulting OLEDs yielded broad structureless emission with a maximum at 640 nm and a green shoulder in the 500−560 nm region (Figure 4). The low-energy band is most likely the same exciplex that is formed by optical excitation of the niBr·Irppy films. The shapes of the quantum efficiency versus current density and current density versus voltage (Figure 7 and Figure 8, respectively) plots are similar to btpIr- and btIr-doped type 1 OLEDs. The type 1 devices reach a maximum quantum efficiency of 0.3% (6.0 V and 20 mA/cm^2). Type 2 devices achieve the same maximum

(51) Baldo, M. A.; Adachi, C.; Forrest, S. R. *Phys. Rev. B* **2000**, *62* (16), 10967.
(52) Lamansky, S.; Kwong, R. C.; Nugent, M.; Djurovich, P. I.; Thompson, M. E. *Org. Elect.* **2001**, *2*, 53.

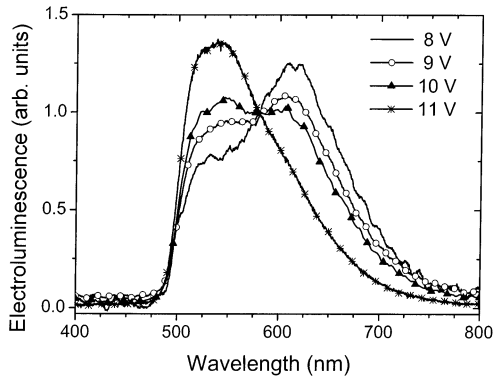

Figure 9. Electroluminescence spectra of a type 2 device doped with Irppy at a range of applied voltages.

quantum efficiency of 0.3%, but at somewhat higher bias than the type 1 device (7.6 V and 6.1 mA/cm^2). The turn-on voltages for both type 1 and 2 devices are ~4.5 V, ca. 1.5 V higher than those of btIr- or btpIr-based devices.

Type 1 Irppy-doped devices show no change in the EL spectrum when the bias is increased. In contrast, type 2 devices showed EL spectra that change dramatically as a function of the applied bias. Figure 9 shows EL spectra of such a device at 8, 9, 10, and 11 V (8, 16, 28, and 44 mA/cm^2, respectively). At low bias values (4−8 V) the device EL spectrum resembled that of the Irppy-doped type 1 device, with a broad emission band in the 600−700 nm region and a weak shoulder in the 500−550 nm region. As the voltage was increased, the green shoulder increased in intensity relative to the red line, and at voltages ≥ 11 V the green band becomes dominant and the red line is a weak shoulder. The dependence of the device EL spectrum on the applied voltage is completely reversible. Voltage-dependent EL spectra are observed only for Irppy-doped type 2 OLEDs. All other OLEDs examined here gave a constant spectrum on changing bias.

The device quantum efficiency for the Irppy-doped type 2 OLED dropped as the bias was increased. The quantum efficiencies for the OLED were 0.27, 0.21, 0.16, and 0.10% at 8, 9, 10, and 11 V, respectively. Inserting ~50 Å of undoped CBP between the Irppy-doped CBP layer and the niBr layer[53] removed the red component of the devices' electroluminescence, making the emission spectra field-independent and identical to that of an OLED emitting from Irppy alone (i.e., green, λ_{max} = 515 nm). This undoped CBP layer, however, did not improve performance of the device (the quantum efficiencies of these devices remained < 0.3%).

Table 3 summarizes the peak device performances of the type 1 and type 2 devices prepared here.

Mechanism of Electroluminescence in niBr-Based OLEDs. Efficiencies of the 1,8-naphthalimide-based OLEDs doped with btpIr are comparable to the efficiencies of the best reported red OLEDs,[10] demonstrating that 1,8-naphthalimides could be utilized as a new class of electron-transporting and hole-blocking materials in red electrophosphorescent OLEDs.

Comparison of electroluminescent and photoluminescent properties of the dopant−host systems presented here allows us to examine the energy-transfer and charge-trapping processes in these OLEDs. The nature of these optical and electronic processes in OLEDs is discussed with reference to the energy diagram of the isolated materials in their flatband conditions, as depicted in Figure 3. Although this is not intended to be a representation of the relevant energy levels under applied bias, it provides a suitable basis for the discussion of the carrier injection, transport, and recombination. The HOMO levels of NPD and each of the Ir dopants are reasonably well aligned, while the barriers for hole transfer from NPD to either niBr or CBP are very large. Thus, it is likely that direct injection of holes from NPD into the dopant molecules is important for both niBr and CBP host devices. The holes in these doped films will be either trapped or carried by the dopant molecules. At the levels of doping used here the average interdopant distances are short and carrier conduction may be facile.[54] On the basis of the energy diagram, we expect the electrons in these devices to be carried by the host matrix for both CBP- and niBr-based devices, since they have lower LUMO energies than any of the dopants used. Hole−electron recombination in these devices is thus expected to involve both the dopant and host molecules, since the hole will be localized on the dopant and the electron on the host. The exciton formed in this process can either be localized on the dopant, as seen for btpIr devices, or form an exciplex, whose wave function covers both the dopant and the host molecule, as seen for Irppy·niBr.

Exciplexes are observed for the niBr·Irppy system, in both electro- and photoluminescent processes. The optical formation of the exciplex involves first the excitation of a single molecule (Irppy or niBr), followed by relaxation of that exciton into the lower energy exciplex state. The exciplex formation pathway used in optical excitation is not likely for the electroluminescently formed exciplex. To follow that type of process, the hole−electron recombination would have to initially lead to either Irppy or an isolated niBr molecule in its excited state, followed by relaxation into the exciplex. Both of these excited states are markedly higher in energy than the resulting exciplex, leading to a thermodynamically unfavorable situation. Thus, it is more likely that the hole−electron recombination leads directly to the exciplex for niBr·Irppy films.

Type 2 Irppy-doped devices demonstrated voltage-dependent spectra (Figure 9). At low voltages, the emission originated from a very efficient exciplex formed between Irppy and niBr (red band). At higher bias levels the emission comes from the Irppy-

Table 3. Summary of Device Performance Data for btpIr-, btIr-, and Irppy-Doped NiBr-Based OLEDs[a]

dopant	device structure	QE_{max} (V at QE_{max}) %, V	$V_{turn-on}$
BtpIr	1	1.7 (6.1)	3
BtpIr	2	3.2 (6.3)	3
BtIr	1	0.4 (5.7)	3
BtIr	2	0.3 (8.9)	4
Irppy	1	0.3 (6.0)	4.5
Irppy	2	0.3 (7.6)	4.5

[a] QE_{max} is the external quantum efficiency (photons/electons), and the turn-on voltage is the voltage at which the light emission from the OLED increases to 10 times the background level (typically 2−5 cd/m^2).

(53) Device structure: ITO/α-NPD (350 Å)/CBP·Irppy (200 Å)/CBP (50 Å)/niBr (100 Å)/Alq_3 (200 Å)/Mg−Ag.

(54) OLEDs prepared with neat films of Irppy as the HTL (ITO/Irppy/luminescent layer/ETL/Mg−Ag) have been prepared and show no HTL emission and low-voltage operation, i.e., similar to the OLEDs described here. At doping levels of 6−8%, chains of dopant molecules with close dopant−dopant contacts are expected in the doped layer, which would have carrier conduction along the chain similar to the neat thin film. These chains could readily conduct holes into the luminescent layer. Adamovich, V.; Thompson, M. E. Unpublished results.

doped CBP layer (green band). This observation suggests that the location of the electron−hole recombination zone in these devices is field dependent, and at low voltages it occurs at the CBP·Irppy/niBr interface and shifts into the CBP layer at higher bias. The Irppy:niBr exciplex could be formed very efficiently when the hole and the electron are localized at Irppy and niBr molecules, respectively. In order for this to happen efficiently, the holes must be localized on Irppy molecules adjacent to the CBP/niBr interface, which is likely since Irppy is the principal hole conductor in these devices. As the voltage is increased, electrons are injected into the doped CBP layer and ultimately recombine at Irppy, leading to an Irppy-based exciton and not the interfacial exciplex.

The current−voltage characteristics for the Irppy type 1 and 2 devices are very different. Significantly less current is passed through the type 2 device at a given voltage than is passed through the type 1 device, Figure 8. Having the carrier recombination confined near the CBP/niBr interface, as it is in the type 2 device, may be the cause of this difference. In the type 1 device, the electrons are injected into niBr and are free to migrate until they recombine with a hole on Irppy or are lost into the hole-transporting layer. In the type 2 devices, the electrons directly recombine with Irppy-based holes near the interface or must be injected into CBP. The latter process is a significant barrier to electron injection and will act to limit the current. The exciplex state is fixed at the CBP/niBr interface, hindering further charge injection. As the bias is raised, electrons are injected into CBP (leading to Irppy emission rather than the interfacial exciplex), but the injection barrier at the CBP/niBr interface remains a limitation to current flow through the device. The fact that the current−voltage plots of the btpIr devices do not show the same behavior suggests that the charges recombine at the dopant, near the CBP/niBr interface, and the btpIr-based exciton is free to migrate into the host matrix.

Among the three different Ir phosphorescent dyes used in this study, only one, namely, Irppy, appears to form an exciplex with the 1,8-naphthalimide host. The three dopants have similar HOMO energies and would be expected to form exciplexes with similar energies. That being the case, it is surprising that the exciplex is only observed for Irppy. Exciplex electronic states have a degree of charge-transfer character; that is, one of the components acts as an electron donor (D), while another behaves as an electron acceptor (A).[55−56] This leads to a correlation between the exciplex emission maxima and the reduction−oxidation properties of the components that make it up. Systematic studies of exciplexes[55] revealed a linear correlation between the emission energy of the exciton at λ_{max} ($E_{exciplex}$) and the solution redox potentials of the components:

$$E_{exciplex} = E(D/D^+) - E(A/A^-) + \text{Constant}$$

where $E(D/D^+)$ and $E(A/A^-)$ are the oxidation potential of the donor component and reduction potential of the acceptor component, respectively. The electrochemical potentials for the donor (Ir-based dopants) and acceptor (niBr) components are listed in Table 2, relative to a common reference (ferrocence). The Irppy excimer ($E_{excimer}$(Irppy) = 2.0 V) is used to estimate the value of the constant in the equation above as 0.13 V, leading to values for the btIr·niBr and btpIr·niBr exciplexes of 2.24 V (561 nm) and 2.04 V (608 nm), respectively.

There are three different energetic situations present for the three dopants in niBr, which lead to the observed spectra and OLED efficiencies. For btpIr, the monomer and exciplex are close in energy and the niBr triplet is much higher in energy. Thus, the lowest energy excited state will either be the dopant alone or the exciplex. On the basis of the spectra and OLED efficiencies it appears that btpIr alone is the preferred site of emission. This could be due to either the btpIr dopant excited state actually being lower in energy than the exciplex (the calculated exciplex energy above is only an estimate) or btpIr having a markedly shorter lifetime than the exciplex. Since the exciplex is not observed, we cannot measure its energy or lifetime to determine which of these is the best explanation. The lower efficiency of type 1 btpIr-based OLEDs relative to type 2 devices may be due to some relaxation through a weakly emissive exciplex state for the type 1 device, which does not occur when the btpIr and niBr are separated in the type 2 device.

The situation for niBr·Irppy is very different. In this case, the Irppy dopant state is the highest in energy, followed by the niBr triplet, and lowest energy excited state is clearly the exciplex. Thus, only exciplex emission is observed and the emission is weak, leading to low OLED efficiencies.

The btIr case is intermediate between these two extremes. The btIr dopant, the niBr triplet, and the exciplex are all of very similar energies. The only emission that is observed is from the btIr dopant alone; however, the device efficiencies were poor. In this device the triplet state of niBr and the exciplex could easily be populated at room temperature, but would not lead to significant emission relative to btIr alone, since the luminescent efficiency for btIr[33] is expected to be significantly higher than either the niBr triplet or exciplex states. Thus, the low efficiency for the niBr·btIr-based devices is most likely due to competing relaxation though poorly emissive states (i.e., niBr triplet or exciplex).

Conclusions

The investigation of the 1,8-naphthalimide derivatives demonstrated that these compounds have charge-transport and film-forming properties, which make them useful materials for utilization in phosphorescence dye doped OLEDs, as hole-blocking and electron-conducting materials. Among the electrophosphorescence dopants we investigated, the 1,8-naphthalimide derivatives are best used for red emissive dopants, i.e., btpIr. Using dopants with higher energies of the luminescent excited state, such as Irppy, leads to efficient generation of a weakly emissive exciplex. Formation of such a charge-transfer state between the Irppy and the 1,8-naphthalimide derivatives is consistent with an analysis of the HOMO and LUMO energies for Irppy and niBr, respectively. A similar analysis suggests that the exciplex states for yellow and red emissive dopants (i.e., btIr and btpIr, respectively) are comparable in energy to the dopant triplet states themselves and may not be efficiently formed. Thus, for btIr and btpIr only dopant emission is observed in either photo- or electroluminescence. While only the btIr emission is observed, nonemissive exciplex and niBr triplet states may have contributed to the excited-state distribution formed in electroluminescence, leading to poor EL ef-

(55) Gilbert, A.; Baggot, J. *Essentials of Molecular Photochemistry*; CRC Press: Boca Raton, 1991.
(56) Gould, I. R.; Young, R. H.; Mueller, L. J.; Albrecht, A. C.; Farid, S. *J. Am. Chem. Soc.* **1994**, *116*, 8189.

ficiency. The conclusion reached here is that the most efficient OLEDs are likely to result from devices in which the phosphorescent dopant alone has the lowest energy excited state (i.e., lower than the triplet of the host matrix or the host·dopant exciplex).

We conclude that the transport mechanism of positively charged carriers in Ir dye doped 1,8-naphthalimides films involves hopping of the holes between dopant molecules. As a result, the electron−hole recombination at the phosphorescence dye molecule is highly probable, making it the dominant mechanism for exciton formation in these devices.

Acknowledgment. We thank the Universal Display Corporation and DARPA for their financial support of this work.

Supporting Information Available: Optical micrographs of doped and undoped naphthalimide films, as well as the cyclic voltammetric traces for niH, niPh, niBr, btpIr, btIr, and Irppy (PDF). This material is available free of charge via the Internet at http://pubs.acs.org.

JA0263588